Archives of Laser and Photonics

Apollonov VV. Arch Laser Photonics: ALP-101.

Review Article

DOI: 10.29011/ALP-101. 100001

High Energy HF (DF) Lasers

Victor V. Apollonov*

Prokhorov General Physics Institute of RAS, Moscow, Russia

***Corresponding author:** Victor V. Apollonov, Prokhorov GPI RAS, Dm. Ulyanov Str.3, ap.147, 119333, Moscow, Russia. Tel:+7 9859207366; E mail: vapollo@kapella.gpi.ru

Citation: Apollonov VV (2018) High Energy HF (DF) Lasers. Arch Laser Photonics: ALP-101. DOI: 10.29011/ALP-101. 100001

Received Date: 27 July, 2018; **Accepted Date:** 15 August, 2018; **Published Date:** 23 August, 2018

Introduction

Non-chain HF (DF) lasers are the most suitable and ecologically safe source of powerful and energetic coherent radiation in the 2.6-3.1 μm (HF laser) and 3.5-4.1 μm (DF laser) spectral regions. Among the different methods of HF(DF) pulse and pulse-periodic laser creation suggested by our team under the guidance of Academician A.M. Prokhorov was self-sustained volume discharge (SSVD). It is well known that a SSVD can be established in a gas by creating a primary electron density that exceeds a certain minimum value n_{min} throughout the discharge gap. Various methods for the pre-ionization of the gas in the discharge gap have been developed for this purpose. Using these methods, primary electrons can usually be created directly in the discharge gas, which sometimes causes difficulties in the establishment of the conditions necessary for the formation of SSVD. For example, high voltages are needed for the formation of an initial plasma when the pre-ionization source and active medium are combined in the same volume, whereas pre-ionization with ultraviolet radiation may be ineffective because of the strong absorption of such radiation in a medium. In the case where soft x-rays are used, it is necessary to ensure rigid synchronization of the x-ray and pump sources.

In the mixtures of gases typical of CO_2 lasers, electron losses due to the trapping process are relatively small at low values of *E/p*. The trapping coefficient is considerably smaller than the absorption coefficient of ultraviolet radiation for the same mixtures. In principle, it should be possible to create primary electrons at the density needed for the formation of a SSVD at a considerable distance from an ionization source, and then to transport the electrons to the gap by drift in an electric field. We have investigated and confirmed this physical matter experimentally [1]. A SSVD formation method that works by filling the discharge gap with a flux of electrons drifting in an electric field, without preliminary ionization of the whole discharge volume, was proposed and implemented by our team. The electron source was a plasma formed in an auxiliary discharge initiated under a grid cathode. This method also made it possible to establish a SSVD in a system with a strongly inhomogeneous electric field in the discharge gap [1].

The basic advantages of non-chain electric discharge HF (DF) lasers are high radiation pulse power, the ability to operate at reasonable pulse repetition frequencies, simple design and convenience of use. This method is one of the most attractive for applications and it is ecologically safe [2]. However, for an appreciable length of time these lasers were limited by their relatively low maximum radiation energy (<10 J). Evidently, the problem of improving the energy characteristics of similar lasers, as with most other electric discharge lasers operating at intermediate and high gas pressures, is readily connected to the challenge of performing SSVD itself. We investigated SSVD in the working mixtures of non-chain HF (DF) lasers with the aim of increasing their radiation energy to at least the level of a few hundred joules [2-12]. As a result of this study, a number of special features were found for non-chain HF (DF) lasers [3-12], which not only follow the traditional principles for forming a volume discharge at intermediate and high gas pressures [13,14], but also largely contradict them. Specifically, it was found that SSVD can be ignited without any preliminary ionization in SF_6 and mixtures of SF_6 with hydrocarbons (deuteron–carbons) [2,3]. We called this form of SSVD self-initiated volume discharge (SIVD) [5]. The realization of SIVD in large volumes allowed us to increase the radiation energy of non-chain HF (DF) lasers up to ~400 J at an electrical efficiency of ~4% [7-11].

An attempt has been made to obtain a deeper insight into the physics of SIVD, starting from the results of the investigations of non-chain HF (DF) lasers that we performed with A.M. Prokhorov at the GPI RAS, and analyze the potential of the method for further increasing the energy parameters of non-chain lasers.

A New Form of SSVD

Certain conditions should be met on the way to SIVD realization in dense gases, the following of which are the basic ones.

(1) Primary electrons with number densities of no less than 10^6-10^9 cm^3 must be created within a gas volume through its preliminary ionization.

(2) In the special case where SSVD is employed for laser excitation, which imposes tight constraints on the uniformity of the active medium characteristics over the working volume, the primary electron multiplication should occur in a uniform electric field, which is usually provided by special shaping of the electrode surfaces.

Clearly, the first condition cannot be observed in such a strongly electronegative gas as SF_6 [5,7] because of the great primary electron losses from electron attachment, except for in the special 'photo triggered discharge' mode [15], which, however, is ineffective for energy input into molecular gases because of the low over-voltages at the gap and, in the case of large discharge gaps and active medium volumes, it is not realized at all. With increasing laser aperture and discharge volume, the problem of how to meet the second condition also arises–there are technical difficulties regarding the fabrication of large-sized intricate-shaped electrodes and the rise of the discharge circuit inductance caused by a useless growth in the transverse size of the electrodes [3,4].

It clearly follows from the simplified analysis presented above that the possibilities for the creation of powerful electric discharge non-chain HF (DF) lasers while following the known physical principles for forming SSVD in dense gases are very limited. Moreover, when starting from these principles, all attempts to create non-chain HF (DF) lasers with a radiation energy of ~1 kJ and above seem to hold no promise. This appeared to restrain researchers' efforts to increase the energy parameters of non-chain HF (DF) lasers. Although there have been numerous works concerned with non-chain HF (DF) lasers, the radiation energy attained for them by 1996 was at the level of 10 J [16-18]. The incompleteness of the traditional understanding of the physics of forming SSVD in dense gases came to be understood after we found that it was possible to obtain discharge in SF_6 and mixtures of SF_6 with hydrocarbons (deuteron-carbons) in the systems of plane electrodes with high electric field enhancement at the edge without any pre-ionization in a gas [2,3]. The sufficient condition for the realization of SSVD in this case was the presence of small-scale (~50 μm) roughness on the cathode. We called this form of discharge SIVD [5]. SIVD is not dissimilar to an ordinary SSVD with pre-ionization. It comprises a set of diffuse channels that diverge in the direction of the anode and attach to bright cathode spots. When overlapped, these diffuse channels show a common diffuse glow [3,5]. The SIVD current and voltage oscillograms are also typical of SSVD in electronegative gases [5]. In non-chain HF (DF) lasers with a rough cathode surface, pre-ionization influences not only the discharge characteristics, but also the output laser energy [3,5]. It should also be mentioned that analysis of the literature data indicates a negligible role for pre-ionization in the formation of SSVD in non-chain lasers. For example, a set of metal rods connected to a common busbar through a resistance (resistance uncoupling) served as the discharge gap cathode, pre-ionization was absent, while in [18] it was performed through a high current dielectric surface discharge whose spectrum displayed not only UV radiation, but also soft x-ray radiation.

We have defined SIVD as a form of SSVD that is obtained without pre-ionization in SF_6 and SF_6 based mixtures under SF_6 pressures of 30-150 Torr, which are typical for HF (DF) lasers. Based on analysis of the experimental results, the following questions are considered below.

(1) What are the key features of the development of SIVD?

(2) What are the physical mechanisms that determine the possibility of SIVD existing?

(3) Is SF_6 a unique gas or can SIVD can be observed in other gases?

(4) What are the active medium and output characteristics of non-chain HF (DF) lasers based on SIVD?

(5) What are the prospects for further increases to the radiation energy of non-chain lasers?

The setup used to investigate the dynamics of SIVD formation is represented schematically in Figure 1. A SIVD of ~500 ns duration was initiated in a SF_6:C_2H_6 = 10:1 mixture at a pressure of 33 Torr and an inter-electrode distance of 4 cm. The electrodes were a 0.5 mm thick and 16 cm long copper stripe (cathode) stood edgewise and a disk anode with a diameter of 6 cm rounded off along its perimeter to a radius of 1 cm. The breakdown was force initiated at the gap edge by a low-current spark restricted by resistance $R = 900\ \Omega$. This spark could not in principle provide a sufficient number of primary electrons in the gas volume, but it allowed the site of the primary gap breakdown to be spatially stabilized. The luminosity of the SIVD was recorded by a single frame camera with an exposure time of 20 ns that was run with varying time delays relative to the instant of the gap breakdown.

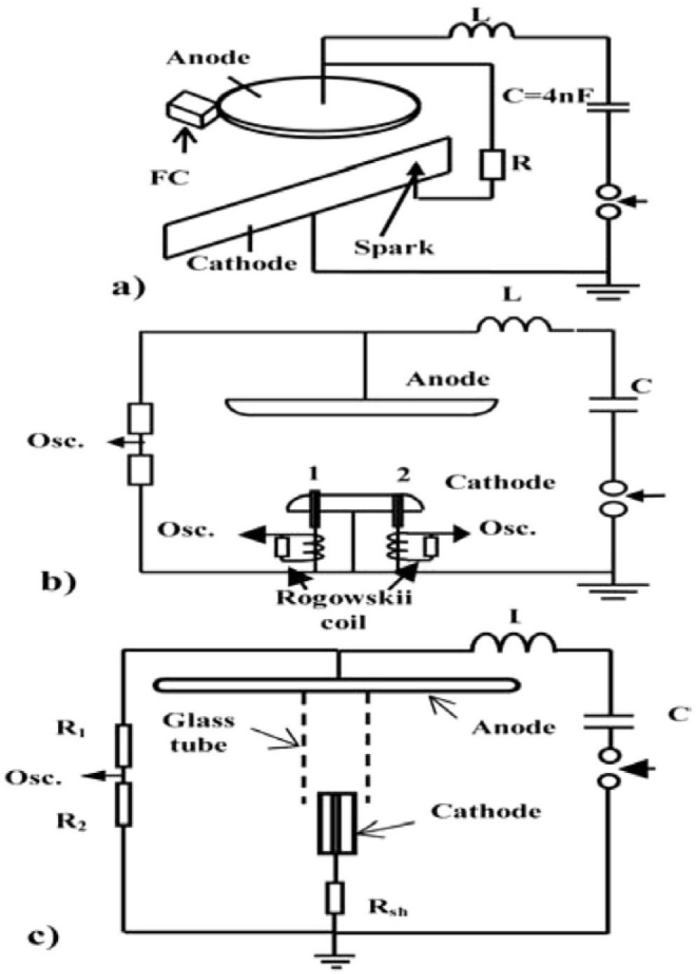

Figure 1: Scheme of the experimental setup for investigation of the SIVD dynamics.

The SIVD dynamics was also studied in the plane-plane gap geometry in experiments with the sectioned cathode depicted in Figure 1.

In this case, the inter-electrode distance, the working medium pressure and the setup's electrical scheme were the same as in the former experiment, but the cathode was a flat disk rounded off along its perimeter to a radius of 1 cm. Isolated conductors with a diameter of 1 mm were inserted into holes with a diameter of 2 mm that had been drilled within the flat part of the cathode and spaced at a distance of ~4 cm. The basic cathode and these conductors were connected to a common bus. The current through each conductor was recorded by Rogowskii coils. One of the conductors (1) extended ~1 mm above the cathode surface, which ensured a primary gap breakdown at that point, whilst comparing the oscillograms for the currents through the initial (1) and control (2) conductors allowed the SIVD extension over the gap to be followed.

The dynamics of a single diffuse channel was investigated using the setup represented schematically in Figure 1. The diffuse channel was initiated via discharge in the rod (cathode) -plane geometry in the SF_6:C_2H_6 = 10:1 mixture at pressures p = 16.5 + 49.5 Torr and an inter-electrode distance of d = 4 cm. The end of a 1.5 mm diameter rod dressed with polyethylene insulation was used as a cathode and the anode was a disk with a diameter 10 cm. Limitation of the cathode surface ensured the development of no more than one cathode spot. The SIVD dynamics was followed by a single frame camera, as in the experiments performed according to the scheme in Figure 1. The SIVD was also filmed with a video camera, which allowed exact calculation of the volume occupied by the discharge as a function of the energy put into the plasma, with the latter being calculated via the current and voltage oscillograms. With the aim of increasing the specific power input into the discharge plasma SIVD in the given gap, the geometry was bounded, in a number of experiments, by a glass tube with a diameter of 6-8 mm (bounded SIVD [6,11]), as shown in Figure.1using a dashed line. This made it possible to bring up specific energy depositions to ~1 J cm^{-3}.

The frames of the SIVD obtained via a single frame camera at different instants of time relative to the instant of the gap breakdown are shown in Figure 2. Figure 3 gives the discharge voltage and current oscillograms that correspond to the process we have described. As can be seen from Figure 2, the gap is broken down at the edge in the vicinity of an auxiliary electrode. At this instant in time, the SIVD constitutes a single diffuse channel with an already developed cathode spot. Then, near the first channel, much less bright new channels appear, which grow temporally in number while their brightness gradually becomes comparable to that of the first channel, with the brightest channel being the one located closest to the primary channel. In time, all the channels become equally bright, while the glow intensity of the first channel decreases noticeably. On further development of the SIVD, an increase in glow intensity is observed for the diffuse channels at the gap edge removed from the region of the first breakdown. However, at T > 250 ns the glow again becomes homogeneous throughout the length of the cathode, with the glow within the region of the first channel being recovered. Further, discharge instability begins to develop against the background of the total glow.

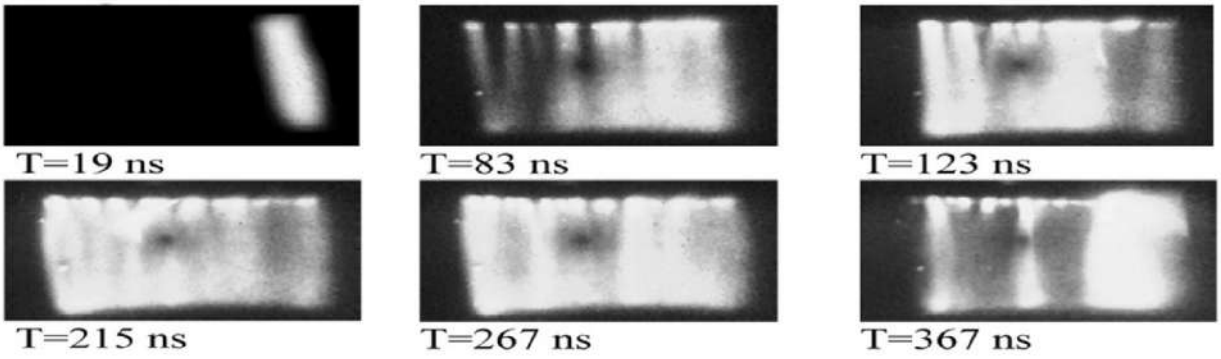

Figure 2: SIVD frames for different *T*-values.

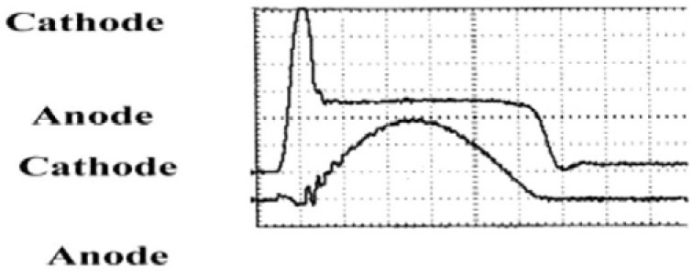

Figure 3: Typical oscillogram for the voltage (upper trace) and current (bottom trace). Timescale: 100 ns div^{-1}.

A very interesting picture of SSVD development is observed. Despite a local gap breakdown and the drop of the voltage across the gap to its quasi-stationary value (see Figure 3), close to that of the static breakdown voltage in SF_6 [19], the initially formed channel is no longer capable of passing all the energy restored in the capacitor through itself, as takes place, for example, in air or nitrogen [7], where a local gap breakdown, even in the form of a diffuse channel, must be followed by discharge instability and, at a sufficiently high restored energy, transition of the discharge from its diffuse to a constricted state. Instead, we see the formation of new diffuse channels after the appearance of the first one, and the extension of SIVD to the whole gap at the voltage close to the static breakdown value (see Figure 3); in so doing, judging from the decrease of the brightness of the first channel in time, the current through it not only rises, but, conversely, falls with the appearance of new channels, i.e. an initially formed channel progressively quenches. It should be noted that the effect of current recovery, which is demonstrated in Figure 2 and manifests itself by equalizing the brightness of all the channels after their initial drop, is only observed under sufficiently high deposited energies. With decreasing energy or cathode size growth (accompanied, naturally, by increased anode size), this effect is absent. However, when high energies are deposited in the discharge plasma (150-200 J l^{-1}), as is typical of HF (DF) lasers, SIVD extends to the whole gap so quickly that the single frame camera we use does not allow the process to be resolved.

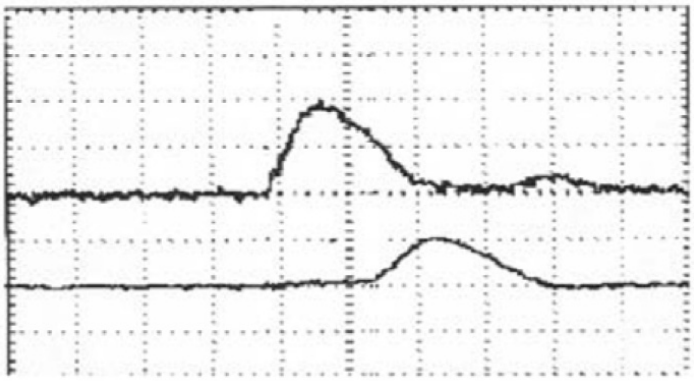

Figure 4: Oscillogram for the current through the initiating (upper trace) and control (bottom trace) wires. The timescale is 50 ns div^{-1}.

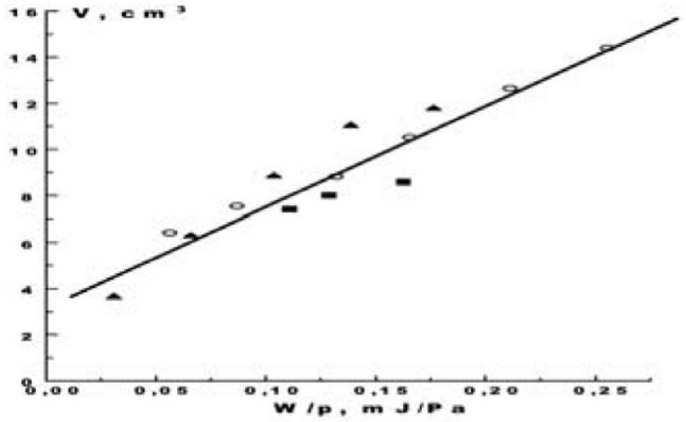

Figure 5: Dependence of volume *V* occupied by SIVD on *W/p*. Mixture: SF_6:C_2H_6 = 10:1. *I–p* = 5 Torr; *A–p* = 30 Torr; and *O–p* = 45 Torr.

A similar picture of SIVD development is observed in the discharge gaps with plane-plane geometry. Figure 4 shows the oscillograms for the currents through the initiating and control conductors (see Figure 1) obtained in the experiment with a sectioned cathode. It is seen from this figure that the current through

a control conductor begins to flow with a noticeable delay relative to the current through the initiating conductor. It is also seen that the amplitude of the current through the initiating conductor has reduced by half by the time that the current through the control conductor appears, i.e. in the given experiment we observe the effect of the quenching of the first channel through the next channels successively filling the discharge gap as they appear. The number of diffuse channels formed during the discharge current pulse duration, as shown in [5,7], is proportional to the specific energy input into the discharge plasma. It is seen in the oscillogram in Figure 4 that the effect of current recovery in the first channel also takes place in the plane-plane discharge gap geometry after its almost complete quenching. In the experiments described above, we observed an increase of the volume occupied by SIVD in the course of the energy input into plasma in the rod-plane geometry, i.e. the discharge volume depended directly on the energy deposited in this volume. Figure 3.5.5 gives the dependence of the volume V occupied by SIVD on the parameter W/p, where W is the energy put into the discharge and p is the gas mixture pressure. It is seen in Figure 5 that the discharge volume grows linearly with the parameter W/p.

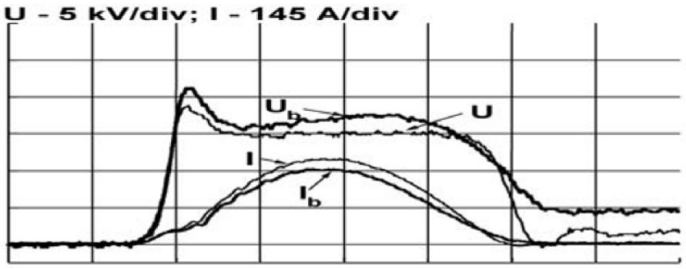

Figure 6: Experimental voltage and current oscillograms for bounded (U_b, I_b) and free (U, I) discharges. Timescale: 50 ns div^{-1}.

After the size of the SIVD in the rod-plane geometry was restricted by a glass tube, the discharge voltage and current oscillograms at energy depositions of up to W_{in} = 200 J l^{-1} showed no changes, but at energy depositions in excess of 400 J l^{-1}, the oscillograms of a bounded SIVD displayed appreciable changes. Figure 6 shows the voltage and current oscillograms for bounded (U_b, h) and unbounded (U, I) SIVD in a SF_6:C_2H_6 = 10:2 mixtures at pressure p = 33 Torr and d = 4 cm. As may be inferred from this figure, on restriction of the SIVD volume (equivalent to increasing a specific energy deposition), the voltage, just after its initial drop under breakdown, rises simultaneously with the current, even during a certain period of time after the current passes its maximum. As a whole, $U_b > U$ whilst $I_b < I$, i.e. an unusual situation is observed here-the gap conductivity decreases with increasing specific energy deposition. It should be pointed out that SF_6 and SF_6 based mixtures are not unique in this respect. Electric discharges in other strongly electronegative gases and their mixtures exhibit similar features. Figures 7 show the current and voltage oscillograms for a bounded SIVD in C_3F_8 and C_2HCl_3:C_2H_6 mixture, respectively. It is seen in Figure 7that the oscillogram U_b shows a more pronounced bend in C_3F_8 than in SF_6.

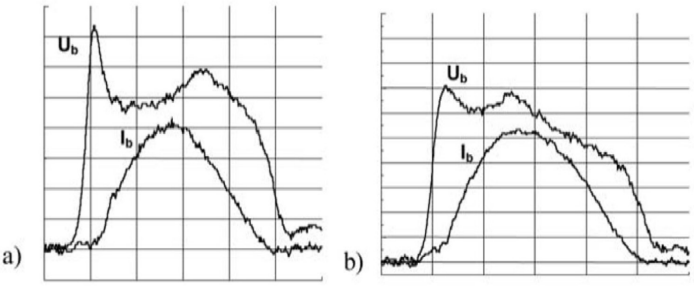

Figure 7: Current (I_b) and voltage (U_b) oscillograms for a bounded SIVD. Timescale: 50 ns div^{-1} (a) – 30 Torr C_3F_8 and (b) mixture: 15 Torr C_2HCl_3 + 3 Torr C_2H_6.

The above-listed features of the development of SIVD allow one to assume that there are current restriction mechanisms in SF_6 and SF_6 based mixtures that make the passage of all the stored energy through a single channel difficult. It is clear that these mechanisms cause the existence of such an unusual form of discharge as SIVD, as well as the possibility of its generation in gaps with a high edge non-uniformity of the electric field. The results presented above are indicative of the presence of certain restriction mechanisms of the current density in diffuse channels in SF_6 and SF_6 based mixtures. It is natural to link the presence of these mechanisms to such a distinguishing feature of SF_6 as its high electronegativity. Relative to other gases capable of attaching electrons to their molecules to form stable negative ions, strongly electronegative gases such as SF_6 are distinguished by (i) the high values of their operating reduced electric fields E/N and (ii) high magnitudes of electro-negativity c_a, defined as the negative ion to electron concentration ratio. This gives rise to some special features for the discharge displays, which we summarize briefly below.

I.) SF_6 molecule dissociation by electron impact becomes important. At E/N-values such that the electron impact ionization coefficient a is no less than the electron attachment rate h, high mean electron energies that approach the SF_6 dissociation thresholds are attained. As a result, more than 80% of the energy deposited goes into dissociation [20]. Note that the dissociative ionization and electron attachment processes characteristic of SFg can contribute significantly to gas decomposition, and specifically to F-atom production [21]. On the sub-microsecond time-scale, the by-products formed have no time to leave the discharge channel, which leads to a local increase in the total gas number density N and, consequently, diminishing electric conductivity.

II.) Because c_a is normally well over unity, large negative ion concentrations are achieved in SIVD, which means that electron generation processes via electron detachment from negative ions may come into play.

Traditionally, detachment processes via negative ion-neutral molecule collisions or/and associative ionization are invoked. However, at intermediate gas pressures (10-100 Torr) on a microsecond timescale, the mechanisms mentioned do not contribute at all to electron multiplication, as follows from experiments and theoretical considerations [22].

On the other hand, there are strong grounds to believe that electron detachment by electron impact may be very efficient at producing secondary electrons in SFg. As applied to the development of electron avalanches in SF_6, this ionization mechanism was first proposed and quantitatively assessed in [23, 24]. It was also later considered for plasmas formed in other fluorine-containing gases.

III. The high positive ion concentrations attained in SIVD, together with the fact that the relation $a \approx h$ holds under the working conditions, mean that dissociative electron–ion recombination can strongly influence the SF_6 discharge plasma parameters, both qualitatively and quantitatively. At the SF_6 plasma decay stage (the trailing edge of the voltage impulse), ion-ion recombination also affects the discharge characteristics considerably. It should, however, be stressed that both of the recombination processes in SF_6 are poorly known, so that no firm data on the corresponding rate constants at elevated reduced electric fields close to $(E/N)_{cr}$ can be found in the literature at this time.

To describe SF_6 dissociation, the energy spent for F-atom production is taken to be equal to 4.5 eV. Further, it is suggested that the negative ion $\mathbf{S}_6^-$ dominates under the conditions of interest, because charge transfer reactions have no time to be accomplished [22] and the cross-sections for the direct production of other negative ions by electron impact are too small [21]. The rate constant for electron impact detachment from negative ions is assessed as $k_d = 10^{-7}$ cm^{-3} s^{-1}, on the assumption that this quantity is no less than that of the elastic electron scattering in SF_6 [23]. The rate constant b_{ei} for dissociative electron-ion recombination is derived with regard to the fact that the positive ion $\mathbf{S}_5^+$ predominates in SF_6 electric discharge plasma [21]. In addition, it is assumed that $b_{ei} \sim T_e^{-1/2}$, where T_e is the electron temperature. As a result, $b_{ei} = 10^{-7}$ cm^{-3} s^{-1} is taken. To determine the ion–ion recombination rate constant b_{ii}, special experiments are carried out [25,26]. Without going into detail, here we give $=10^{-8}$ cm^{-3} s^{-1} as an adequate value for the conditions of interest. It is clear that all the processes considered above, when taken into account with their actual rate constants, may influence the SIVD voltage oscillograms considerably. It can be inferred that dissociative electron-ion recombination and electron detachment by electron impact seem to equilibrate each other, at least within the accuracy to which the corresponding rate constants are presently known. This seems to lend additional support to the estimates for the rate constants k_d and b_{ei} presented in this chapter.

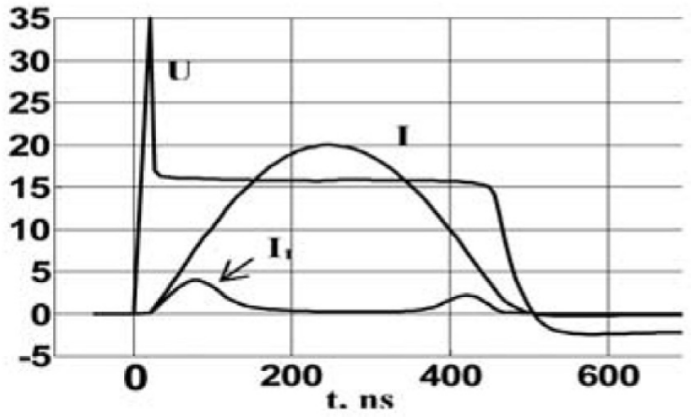

Figure 8: Oscillograms for voltage *U* and general current *I,* and the current through the first channel I_b scales: current-25 A div^{-1}, voltage-5 kV div^{-1} and time-200 ns div^{-1}.

Advanced studies on a sub microsecond intermediate pressure SIVD in SF_6 and SF_6-C_2H_6 mixtures are presented. It is found that the decomposition of SF_6 molecules-either immediately through electron impact or

through dissociative ionization and electron attachment-influences the discharge characteristics (specifically the voltage and current oscillograms) greatly. The breakup of C_2H_6 molecules may also be thought of as a notable dissociation mechanism. Electron-ion dissociative recombination and electron impact detachment from negative ions are felt to balance each other in pure SF_6 and in SF_6 with small C_2H_6 additives. The considered processes enable one to explain such a unique phenomenon as SIVD qualitatively.

It should also be noted that electron detachment from negative ions because of electron impact is one of the most probable mechanisms for the development of SSVD instability in SF_6 and SF_6 based mixtures. Taking into account the influence of the listed processes enables one to describe the dynamics of SIVD formation qualitatively. In our calculations the channel structure of SIVD is modeled by a set of paralleled pure resistances whose conductivity is determined in accord with [10,19]. The differences in the initial conditions when developing the channels lengthwise of the cathode are specified by different initial electron number densities n_0 for each of the channels. A total of nine channels are taken into account, which corresponds to using a knife cathode in the experiment. Figure 8 gives the calculated oscillograms for voltage *U,* total current *I* and the current through the first channel. It is seen that a current through an individual channel displays two maxima, which correlates qualitatively with the results of the experiments that investigated the SIVD dynamics, wherein the effect of current recovery was observed.

By this means, it is the presence of the mechanisms that restrict current through a conducting channel that makes it possible to form SSVD without pre-ionization-SIVD. However, a sufficiently high uniformity and stability should also be ensured for

SIVD to be used in non-chain HF (DF) lasers.

SIVD can only conventionally be assigned to ordinary volume discharges. A volume nature is attained for SIVD by overlapping individual diffuse channels attached to cathode spots, i.e. in principle SIVD has a jet structure. What is important for the uniformity and stability of such discharges is, therefore, not the initial electron number density as such, but the surface density of the cathode spots, which is to a large extent determined by the surface state, in addition to a number of other factors. The results of experiments performed with the aim of revealing these factors are discussed below.

Experiments were carried out in a dielectric discharge camera filled with a mixture of SF_6 and hydrocarbons (C_2H_6 or C_3H_8) at a total pressure of p = 5 + 15 Torr. A volume discharge was burnt between an A1 Ø6 cm cathode rounded off to a radius 1 cm along its perimeter and an A1 Ø12 cm anode at values p_d = 0.02-0.7 cm atm. In the experiments we used both cathodes that had been polished and cathodes that had been subjected to sandblasting. A capacitor was discharged through the gap. Changing the capacitance and the capacitor's discharge voltage varied the energy inserted into the SIVD plasma.

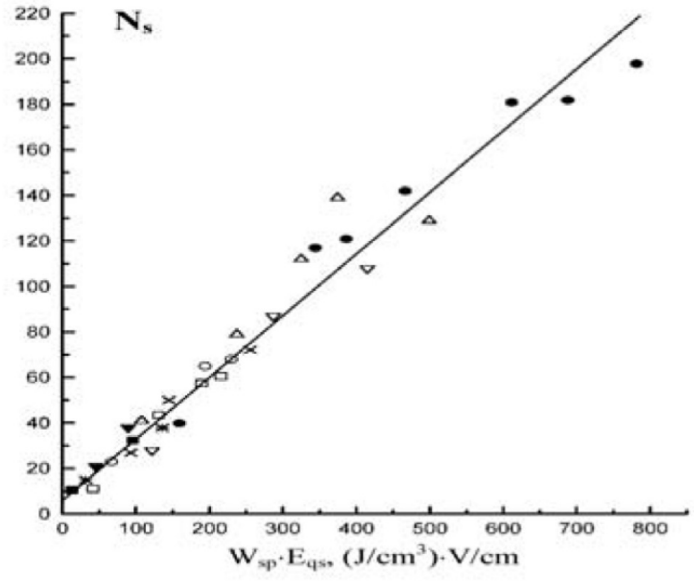

Figure 9: Dependence of the number of cathode spots N_s on $W_{sp}E_{qs}$ for the SF_6: C_2H_6 = 10:1 mixture with d = 6 cm and p = 33.6 Torr (□), d = 6 cm and p = 16.8 Torr (■), d = 4 cm and p = 23.3 Torr (*), d = 3 cm and p = 23.3 Torr (□), d = 3 cm and p = 33.6 Torr (o), d = 3 cm and p = 50.4 Torr (Δ), d = 3 cm and p = 67.2 Torr (•), and d = 2 cm and p = 33.6 Torr (x).

Figure 9 shows the number N_s of spots on the cathode that had been subjected to sandblasting as a function of the parameter W_{sp}, E_{qs}, W_{sp} is the deposited energy per unit gas volume and E_{qs} is the electric field strength in the quasi-stationary phase of SIVD. As can be seen in Figure.3.6.9, this relationship is satisfactorily approximated by a linear function:

$$N_s = a + bW_{sp} - E_{qs}. \quad (1)$$

The rise of the quantity N_s and, consequently, of the cathode spots surface density-which is observed not only when a specific energy deposition is increased, but also when the electric field strength is-reflects the fact that the electric field strength magnitude determines the probability of the formation of a cathode spot to a considerable extent [14]. The constant b in expression (1) is in turn a function of the cathode surface state and the hydrocarbon content in the mixture.

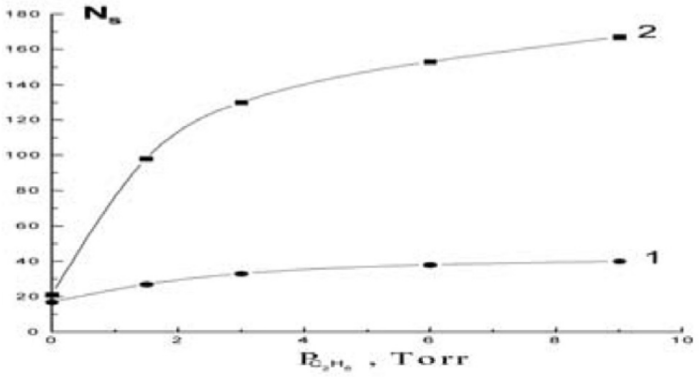

Figure 10: Dependences of the cathode spots number N_s on a partial pressure of C_2H_6 in SF_6:C_2H_6 mixture. SF_6 pressure p = 30 Torr. 1-polished cathode and 2-cathode subjected to sandblasting.

Figure 10 shows the dependences of N_s on a partial pressure of C_2H_6 in the mixture at an SF_6 pressure of 30 Torr while d = 4 cm, obtained using a polished cathode (curve 1; a mechanical polish of the surface is followed by aging via approximately 100 discharges) and a cathode subjected to sandblasting (curve 2). These dependences were obtained at constant energy depositions in the SIVD plasma. As is seen in Figure 10, the quantity N_s increases appreciably with increasing hydrocarbon partial pressure. From this figure it is also evident that the roughness of the cathode surface comes to play a role in increasing the density of the cathode spots and, correspondingly, the effective volume occupied by the SIVD. In accordance with expression (1), the density of the cathode spots in the SF_6-C_2H_6 mixture can also be increased by stepping up the discharge burning voltage through adding small quantities of gases that are more electronegative than SF_6, for example, CCl_4 or C_2HCl_3. Note that 2 Torr C_2HCl_3 addition to the SF_6-C_2H_6 mixture does not lead to a noticeable decrease in the SIVD stability.

The problem of increasing the stability of SIVD in SF_6 based mixtures is adequately covered in [5-10], and so it is not covered in detail in this paper. We only report on the basic results in this area. In [5], it was shown that the addition of hydrocarbons and deuteron-carbons to SF_6 allows specific energy depositions to be increased by a factor of 5-6 at a given discharge duration, for which

reason it is preferable to employ these hydrogen (deuterium) donors in a non-chain HF (DF) laser, rather than H_2 and D_2.

In addition, it was shown in [8,10] that the stability of SSVD in a mixture of SF_6 with hydrocarbons or deuteron-carbons does not in practice depend on whether there are sites of local electric field enhancement at the discharge gap, which enables us to use identical flat electrodes rounded off to small radii $r << d$ along the perimeters as the anodes and cathodes-i.e. to employ essentially compact electrodes-in non-chain HF (DF) lasers. This makes it possible to substantially decrease the size of the discharge camera and, correspondingly, the discharge circuit inductance, which is of great importance in scaling the characteristics of non-chain HF (DF) lasers.

We should point out that the detachment of electrons from negative ions, which is taken into account by us when considering the mechanisms of electric current density restriction, may be one of the possible mechanisms leading to the development of instability in SF_6 and SF_6 based mixtures. However, such an analysis is very challenging because of the severe difficulty of exactly accounting for the plasma composition within the channel growing from a cathode spot, wherein the initial components of the working mixture are strongly dissociated owing to great current densities (up to 10^4 A cm^{-2}).

Non-Chain HF (DF) Lasers Pumped by SIVD

SIVD has great potential for the creation of extremely simple and compact non-chain HF (DF) lasers. However, in the absence of pre-ionization, setups with working medium volumes of less than 21 at a relatively small cathode surface exhibit an appreciable scatter in the pulse breakdown voltage amplitudes that is especially undesirable under the pulse-periodic working mode. Therefore, in the given case, it is expedient to initiate SIVD by, for example, a low-current spark located either outside the discharge gap or in a hole on the cathode [5]. In principle, this regime is similar to a 'photo triggered discharge' mode [15,17,27]. However, in classical photo triggered discharge schemes being applied to excimer lasers, a powerful illumination of the gap is necessary, since this illumination serves the dual function of initiating the breakdown and producing the necessary primary electron number density in a gas medium. In mixtures of SF_6 with hydrocarbons, powerful illumination is not needed, because the distinguishing feature of SIVD is that a discharge after a local gap breakdown spreads, as shown above, over the whole surface of the cathode, wherever it first occurs [5]. This means that a local illumination of the cathode by a low-current spark is quite sufficient to stabilize the electric and output characteristics of HF (DF) lasers. With reference to an unusual operating mode, some special features of an HF (DF) laser with an aperture of 5 cm are considered in this section in detail.

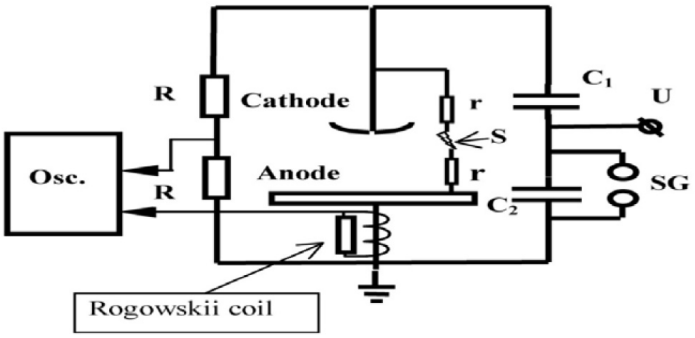

Figure 11: Electrical scheme of the non-chain HF (DF) laser.

In the laser (Figure 11), flat A1 electrodes with dimensions of 20 x 80 cm (anode) and 7 x 60 cm (cathode), rounded off to a radius of 1 cm in their perimeters and separated by a distance of d = 5 cm, were used. The cathode surface was subjected to sandblasting. To obtain SIVD, the Fitch scheme was used with capacitors C_1 and C_2 of 0.1 F and a maximum discharge voltage of 50 kV. The discharge gap was laterally illuminated with a spark limited by two resistances of r = 5 kΩ connected directly to the electrodes.

The spark was located symmetrically relative to the electrodes at a distance of ~5 cm from the cathode edge. Ten blowers ensured the operation of the laser in a pulse-periodic regime with a frequency of up to 10 Hz. The laser worked with mixtures SF_6-C_2H_6 and C_6D_{12} at pressures of 45-70 Torr. In the majority of the experiments, a resonator formed by an A1 mirror with a radius of curvature of 20 m and a plane-parallel plate of BaF_2 was used. The laser radiation divergence was measured using an unstable telescopic resonator with the amplification M = 3. To rule out the influence of the near-electrode regions on the results, the laser aperture in these measurements was limited to a diameter of 4 cm. The radiation divergence measurements were carried out via the focal spot method using a mirror wedge [28].

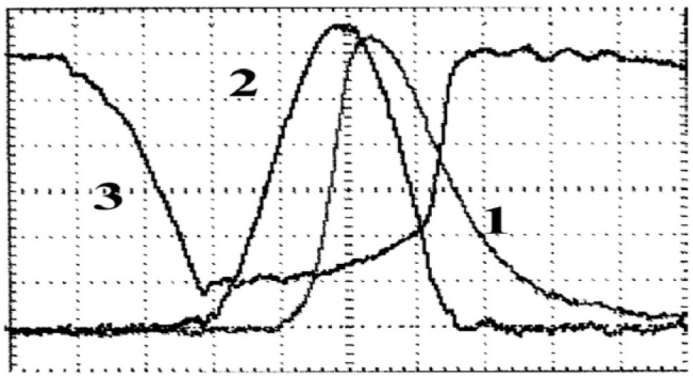

Figure 12: Typical oscillogram of laser pulse (1), current pulse (2) and voltage across the discharge gap (3) for the mixture 66 Torr SF_6 + 6 Torr C_2H_6. Scales: current-3 kA div^{-1}, voltage-10 kV div^{-1} and time-100 ns div^{-1}.

Note that in contrast to a typical photo triggered discharge system, breakdown initiation in our case occurred spontaneously as soon as the voltage across the gap exceeded a certain critical magnitude. With the separation of the illumination scheme from the laser-pumping scheme, it was possible to initiate breakdown at an arbitrary instant of time.

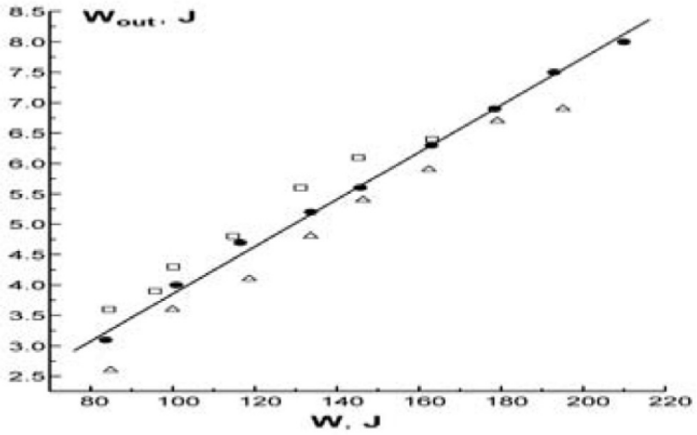

Figure 13: Dependences of the output laser energy (W_{out}) (generation on HF) on energy W deposited in the discharge plasma obtained for mixtures of C_2H_6:SF_6 with different component ratios: □-1:22, ●-1.5:22 and Δ-2:22.

Typical oscillograms for the pulses of the laser generation, current and voltage across the gap are presented in Figure 12 (curves 1, 2 and 3, respectively). As is seen in this figure, discharge gap breakdown occurs due to photo initiation at the leading edge of the voltage pulse, a laser pulse maximum delaying slightly relative to the current maximum.

Without the initiating spark, the scatter in the gap breakdown voltage amplitudes is as high as 20%, which, correspondingly, causes a spread of 15% in the magnitudes of the output laser energies. Figure 13 shows the dependence of the output laser energy (W_{out}) (generation on HF) on the energy W deposited in the discharge plasma for mixtures with different proportions of C_2H_6. It can be seen that in the mixtures with the component ratios C_2H_6:SF_6 = 1.5:22 and 2:22 the output energy rises with the increase of the deposited energy practically linearly. In the experimental conditions, the mixture C_2H_6: SF_6 = 1.5:22 turned out to be optimal, with a maximum value of the generation energy of W_{out} = 8 J obtained at an electrical efficiency of 3.2%. The discharge volume assessed by the laser radiation print on thermal paper was -1.51, which corresponds to a specific energy deposition in the plasma of ~220 J l^{-1}. A decrease of W_{out} with increasing W in mixtures with a lower content of C_2H_6 (mixture C_2H_6:SF_6 = 1:22) arose from discharge instability at high energy depositions.

Indeed, in this mixture, when operating at energy depositions of ~200 J l^{-1}, we observed bright plasma stems growing from the cathode edge, which sometimes bridged the gap. For mixtures with a higher C_2H_6, content, there was no decrease in laser efficiency with increasing W until the discharge remained stable, and the lengths of the plasma channels were not in excess of $d/2$. This causes us to anticipate that the increase of the electrical efficiency with increasing inter-electrode distance takes place because the SIVD becomes more uniform due to a greater overlapping of diffuse channels [5,7].

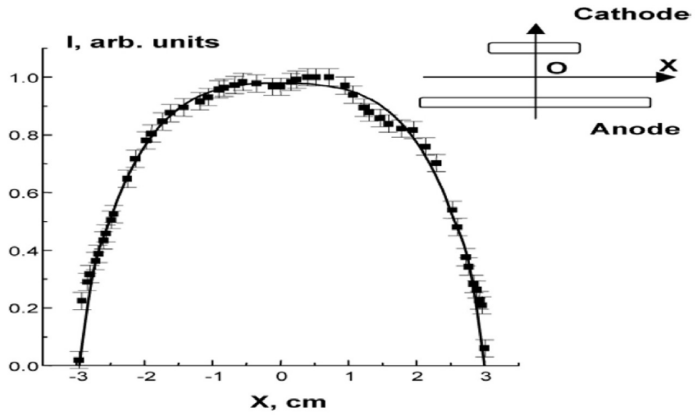

Figure 14: Plasma intensity distribution over the optic axis-contained plane placed in parallel to the electrode surfaces.

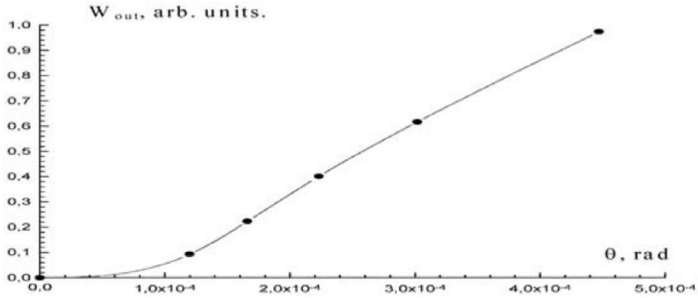

Figure 15: Angular distribution of the radiation energy in the far zone.

In the investigated electrode system, a great enhancement of the electric field takes place at the gap edge. In such gases as CO_2, air and N_2, this results in the discharge concentrating at the gap edge [4]. In mixtures of SF_6 with hydrocarbons this is not the case, because of the distinguishing feature of SIVD-even though SIVD originates at the edge, it then displaces into the interior of the gap because of the existence of the mechanisms that limit the current density in a diffuse channel. The SIVD plasma intensity distribution over the optic axis-contained plane parallel to the electrode surfaces is shown in Figure 14. The maximum of the SIVD luminosity intensity is attained at the axis. The radiation energy is also distributed over the laser aperture in a similar manner, i.e. the edge's electric field enhancement does not appreciably influence the distribution of the output laser radiation.

By this means, a local illumination of the cathode is quite sufficient to obtain a uniform SSVD in mixtures of SF_6 with hy-

drocarbons, and the presence of regions displaying high edge non-uniformity does not worsen the SIVD stability and only influences the distribution of the laser radiation energy over the aperture slightly.

Therefore, it is possible to use plane electrodes rounded off to small radii along their perimeters. We have not found any appreciable features for the P-P operating mode that have not been mentioned previously elsewhere [27-29].

The radiation divergence was measured in the special case where the laser operated on DF molecules (Figure 15). As can be seen from Figure 15, the radiation divergence at a level of 0.5 is $\theta_{0.5} = 2.9 \cdot 10^{-4}$ rad, which corresponds to four diffraction limits. Further improvement of the given parameter can be expected from increasing the laser aperture, because lengthening the inter-electrode distance should improve the discharge uniformity through greater overlapping of diffuse channels.

Wide Aperture Non-Chain HF (DF) Lasers

On increasing the cathode surface and active medium volume, the necessity of initiating the gap breakdown disappears. In this case, the breakdown delay becomes so negligible that it cannot be inferred from the oscillogram, and the breakdown occurs at the voltage leading edge. Therefore, when dealing with setups with great active medium volumes, there is no necessity for additional units to initiate the gap breakdown, since a sufficiently uniform discharge forms spontaneously.

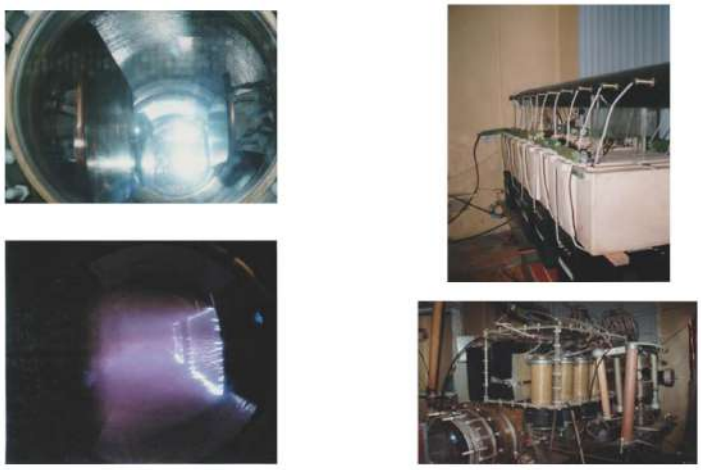

Figure 16: Discharge gap and power source for a non-chain HF laser with P = 407 J.

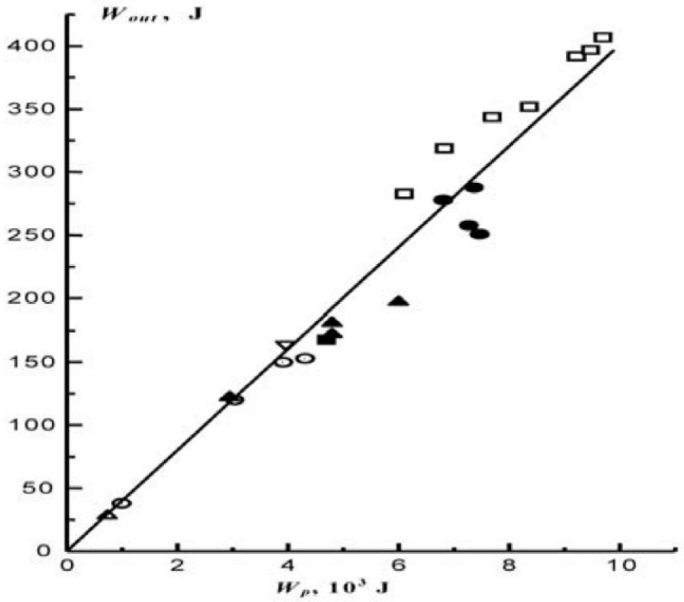

Figure 17: Dependence of the output HF laser energy W_{out} on the energy stored in the generator's capacitors.

We considered the scaling problems for non-chain HF (DF) in previous papers [6,8,10] in greater detail.

Conclusions

So, in this chapter we touch on the necessary conditions for obtaining SIVD in large volumes.

(1) The cathode surface should posses a small-scale (~50 m) roughness.

(2) It is important to match the circuit wave impedance to the discharge plasma resistance at a given inter-electrode distance, and a mixture pressure should be chosen in such a way that the discharge burning voltage determined by the conditions of the gap breakdown in SF_6 [19] is two times smaller than the voltage fed to the gap.

(3) The increase of electrical energy produced via the increase in the generator's capacitance at a given maximum generator voltage should be followed by the growth of the discharge volume V as $V \sim C^{3/2}$, where C is the generator's capacitance [8,10]. On fulfillment of all these conditions, one should also try to maximally decrease the time period of the energy deposition in the discharge plasma.

The maximum generation energies obtained for non-chain HF (DF) lasers in our experiments were 407 J (HF) and 325 J (DF), with electrical efficiencies of 4.3% and 3.4%, respectively. The active medium volume was ~60 l at an aperture of 27 cm (Figure 16). Such a laser with some additional hardware can be pulse-periodic with a repetition rate about 100 Hz., which is important for realization of new set of technologies [30 -32].

Of natural interest is the problem of further increasing the laser radiation energy. Figure 17 shows the dependence of the output HF laser energy W_{out} on the energy W_p stored in the capacitors of a high-voltage generator. This figure reflects the data we obtained using setups with different volumes of active medium. This allows us to predict the possibility of further increases to the output energy of non-chain HF (DF) lasers through the creation of setups that operate at energy depositions above a few tens of kJ using the methods we developed during that very productive period of time [33,34].

References

1. Apollonov VV (1985) SSVD in CO_2-N_2-He gas mixtures. Proc Int Conf Lasers 85: 681.
2. Apollonov VV (2003) SSVD based chemical lasers. Laser Focus World 12: 84.
3. Apollonov VV, Yu Kazantsev S, Oreshkin VF, Firsov KN (1997) Feasibility of increasing the output energy of a non-chain HF (DF) laser. Quantum Electronics 27: 3.
4. Apollonov VV, Yu Kazantsev S, Oreshkin V F, Firsov KN (1998) Non-chain electric discharge HF (DF) laser with high radiation energy. Quantum Electronics 28: 123.
5. Apollonov VV, Yu Kazantsev S, Oreshkin V F, Firsov KN (1998) High-power non-chain HF (DF) lasers initiated by SSVD. Proc of SPIE, XII Int Symp on Gas Flow and Chemical Lasers and High-Power Laser Conf 3574: 374.
6. Apollonov VV (1998) SSVD based pulse non-chain HF (DF) laser. Proc of SPIE, High-Power Laser Ablation 3343: 783.
7. Apollonov VV, Belevtsev AA, Yu Kazantsev S, Saifulin AV, Firsov KN (2000) SIVD in non-chain HF lasers based on SF_6-hydrocarbon mixtures. Quantum Electron 30: 207.
8. Apollonov VV (2000) SSVD for initiated wide aperture non-chain HF (DF) lasers. Izv RAN Ser Fiz 64: 1439.
9. Apollonov VV, Belevtsev AA, Yu Kazantsev S, Saifulin AV, Firsov KN (2000) SSVD in mixtures of SF_6 with hydrocarbons to excite non-chain HF lasers. Proc of SPIE, Int Conf on Atomic and Molecular Pulsed Lasers III 4071: 31.
10. Apollonov VV, Yu Kazantsev S, Saifulin AV, Firsov KN, Oreshkin VF (2000) Scaling up of non-chain HF (DF) laser initiated by SSVD. Proc of SPIE, High-Power Lasers in Energy Engineering 3886: 370.
11. Apollonov VV (2001) Generation and properties of SSVD in strongly electronegative gases. Proc of XXV Int Conf on Phenomena in Ionized Gases, ICPIG-2001 1: 255.
12. Apollonov VV (2001) Volume discharge in SFj mixtures with hydrocarbon's. Proc of XIII Int Conf on Gas Discharge and their Applications, GD-2000 1: 409.
13. McDaniel E W, Nighan W L (1982) Gas lasers. Applied Atomic Collision Physics 3 .
14. Korolev Yu D, Mesyats GA (1991) Physics of Pulse Discharge in Gases.
15. Brunet H (1990) Pulsed HF chemical laser using a VUV photo triggered discharge. SPIE, VIII Int Symp on Gas Flow and Chemical Lasers 1397: 273.
16. Pummer H, Breitfeld W, Wedler H, Klement G, Kompa KL (1973) Parameter study of 10-J hydrogen fluoride laser. Appl Phys Lett 22:319.
17. Puech V, Prigent P, Brunet H (1992) High-efficiency, high-energy performance of a pulsed HF laser pumped by photo triggered discharge. Appl Phys B 55: 183.
18. Burtsev NN (1984) On simultaneous formation of volume and sliding discharges of milli microsecond duration for gas lasers pumping. Proc of VII All-Union Conf on Phys Low- Temperature Plasma (Tartu).
19. Apollonov VV (1987) Discharge characteristics of a non-chain HF (DF) laser. Quantum Electronics 30: 483.
20. Slovetskii DI, Deryugin AA (1987) Electron energy distribution functions and interaction of electrons with polyatomic molecules of fluorine-containing gases. Plasma Chemistry 13: 240.
21. Nakano N,Shimura N,Petrovic ZL,Makabe T (1994) Simulation of RF glow discharges in SF_6 by the relaxation continuum model: physical structure and function of the narrow-gap reactive-ion etcher. Phys Rev E 49: 4455 .
22. Hilmert H, Schmidt W (1991) Electron detachment from negative ions of sulfur hexafluoride-swarm experiments. J Phys D Appl Phys 24: 915.
23. Belevtsev AA, Biberman LM (1997) On a certain nonlinear effect in development of electron avalanches in electronegative gases. Izv Akad Nauk SSSR Energy Transp 6: 74.
24. Hayashi D, Nakamoto M, Takada N, Sasaki K, Kadota K (1999) Role of reaction products in F-production in low-pressure, high-density CF_4 plasmas. Japan J Appl Phys 38: 6084.
25. Apollonov VV,Belevtsev AA, Yu Kazantsev S, Saifulin AV, Firsov KN (2001) Ion-ion recombination in SF_6 and SF_6-C_2H_6 mixtures for high values of E/N. Quantum Electronics 31: 629.
26. Apollonov VV (2001) Ion-ion recombination in SF_6 and SF_6-C_2H_6 mixtures at high values of E/N. Proc of XXV Int Conf on Phenomena in Ionized Gases, ICPIG-2001 3: 277.
27. Lacour B (2000) High average power HF (DF) lasers. Proc of SPIE, III Int Conf on Atomic and Molecular Pulsed Lasers 4071: 9.
28. Abrosimov Yu.M (1982) Measuring of a divergence of a pulsing laser radiation by a method of a focal spot with application of a reflecting wedge. Tech Measure 4: 30.
29. Velikanov SD, Zapol'skii AF, Frolov YN (1997) Physical aspects of the operation of HF (DF) lasers with a closed active-medium replacement cycle. Quantum Electron 27: 11.
30. Apollonov VV (2001) Prokhorov A M Ecologically safe high-power lasers Keynote address. Int Conf Lasers Tucson AX USA.

31. Apollonov VV (2014) Sil`nov S M High Energy/Power P-P Lasers, NOVA.

32. Apollonov VV (2016) High Energy/Power Lasers in Our Life, NOVA.

33. Apollonov VV (2004) High power self-controlled volume discharge based molecular lasers. Opt Eng 43: 16-33.

34. Apollonov VV (2016) High Energy Molecular Lasers. Springer.